Science of the Total Environment 660 (2019) 1245–1255

Contents lists available at ScienceDirect

Science of the Total Environment

journal homepage: www.elsevier.com/locate/scitotenv

Increase in severe and extreme soil moisture droughts for Europe under climate change

Manolis G. Grillakis

School of Environmental Engineering, Technical University of Crete, Chania, Greece

HIGHLIGHTS

- This study found indications about reduction in future soil moisture for Europe under RCP2.6 and RCP6.0.
- It was found that drought events are expected to increase regardless the emission scenario.
- Increase in European severe and extreme soil moisture drought events were projected.
- Drastic increase in soil moisture droughts over 10^6 Km^2 under RCP2.6 and RCP6.0.

GRAPHICAL ABSTRACT

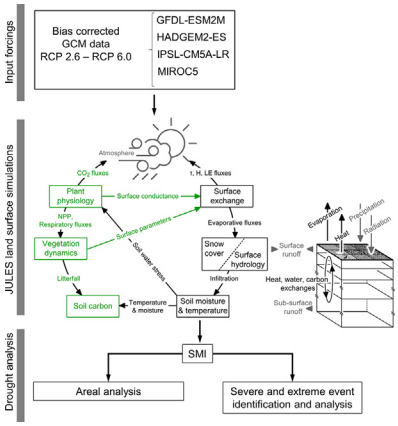

ARTICLE INFO

Article history:
Received 15 September 2018
Received in revised form 31 December 2018
Accepted 1 January 2019
Available online 4 January 2019

Keywords:
Soil moisture index
Soil moisture droughts
JULES land surface model
Drought events identification
Agricultural drought projections
Severe and extreme soil moisture droughts

ABSTRACT

Droughts are among the costliest natural disasters. They affect wide regions and large numbers of people worldwide by tampering with water availability and agricultural production. In this research, soil moisture drought trends are assessed for Europe using the Soil Moisture Index (SMI) estimated on Joint UK Land Environment Simulator simulations under two Representative Concentration Pathways, the RCP 2.6 and RCP 6.0 scenarios. Results show that SMI drought conditions are expected to exacerbate in Europe with substantial differences among regions. Eastern Europe and Mediterranean regions are found to be the most affected. Spatially and temporally contiguous regions that exhibit SMI of Severe and Extreme index categories are identified as distinct drought events and are assessed for their characteristics. It is shown that even under strong emissions mitigation, these events are expected to increase in occurrence (22% to 123%), while their characteristics will become more unfavorable. Results indicate increase in their spatial extend (between 23% and 46%) and their duration (between 16% and 48%) depending on the period and the scenario. Additional analysis was performed for the exceptionally wide-area (over 10^6 km^2) severe and extreme soil moisture drought events that are expected to drastically increase comparing to the recent past. Projections show that those events are expected to happen between 11 and 28 times more frequently depending on the scenario and the period with a 59% to 246% larger duration. These findings indicate that even applying strong mitigation measures, agricultural drought risk in Europe is expected to become higher than our present experience.

E-mail address: manolis@hydromech.gr.

https://doi.org/10.1016/j.scitotenv.2019.01.001
0048-9697/

1. Introduction

Climate change is expected to affect almost every environmental and societal aspect. Socio-economic sectors, from energy (Jacob et al., 2018a), to services (Grillakis et al., 2016b; Koutroulis et al., 2018b), ecosystems (Williges et al., 2017) and water resources (Koutroulis et al., 2018c; Betts et al., 2018), will face unequivocal increase in vulnerability due to changes in climate. Water cycle is one of the most important component of the natural system and one of the most vulnerable from a socioeconomic perspective. Already a large proportion of the world's population is experiencing water stress (Vörösmarty et al., 2000) and hence changes in water availability cause significant impacts. The water stored in the soil is one of the most important water resources, as it sustains a large proportion of the global food production, as rainfed areas account for the 75% of the total global harvested areas (Portmann et al., 2010).

Comprehending soil moisture dynamics in the water cycle and the effect of global warming to it, is of critical importance in order to project and mitigate potential impacts in agriculture. Soil moisture is the amount of water contained in the unsaturated soil layer (Seneviratne et al., 2010). This water storing layer is an integral and dynamic part of the hydrologic cycle. Soil is the first earth component to interact with the atmospheric meteorological phenomena, receiving precipitation and conveying it in deeper ground or atmosphere via evaporation. Soil water dynamics are controlled by nonlinear interactions among different hydrometeorological and biophysical processes that control precipitation, evapotranspiration and runoff (Ghannam et al., 2016). These interactions constitute soil moisture a regulatory agent of plant growth and nutrient uptake (Daliakopoulos et al., 2016), affecting water, energy and biogeochemical cycles (Seneviratne et al., 2010) and even regulates natural hazard phenomena (Grillakis et al., 2016a). It is estimated that >2 billion people have been affected by droughts in the 20th century and have caused 11 million deaths (Spinoni et al., 2014).

Soil moisture drought is the forefront drought issue as it directly affects the plant growth and agricultural crop yields (Ciais et al., 2005) and so is also referred to as agricultural drought. Agricultural drought is the consecutive state after the deterioration of vegetation and ecological health of a region, which comes in turn of the low root zone soil moisture as a result of the enhanced evapotranspiration (Otkin et al., 2018). The environmental, societal and economic impacts related to the soil moisture droughts can become severe, as they often accumulate slowly over a considerable period of time and may persist for years beyond the termination of the precipitation drought (Vrochidou et al., 2013). Rapid decrease in the soil moisture or anomalous low soil moisture conditions, in combination with short periods of warm surface temperature can trigger flash droughts (Otkin et al., 2018). Concurrently, long-lasting droughts and hence soil moisture deficits can result to the lowering of groundwater or surface water reservoir levels (Naumann et al., 2018). The 2003 European summer heat wave in combination to the antecedent prolonged drought period, caused a wide crop shortfall in parts of Southern Europe of a compound cost of almost EUR 15 billion (García-Herrera et al., 2010; Kurnik, 2017). In the late 2018, parts northern and central Europe were facing a period of unusually hot weather that has led to record-breaking temperatures and drought. Farmers were facing crop failure as one of the most intense regional droughts in recent memory strengthened its grip (The Guardian, 2018), with similarities to the 1976's great drought (Marsh et al., 2007) that severely affected UK. According to the media, 2018 drought has caused the most severe problems to the EU vegetable sector in the last 40 years (Euractiv, 2018). In the recent past, Europe has experienced many drought events, not only in the semi-arid regions of Iberian Peninsula and the Mediterranean regions, but also in almost entire territory, from Western to East Europe, and to as high as Scandinavia. Spinoni et al. (2015), provide an analysis of the biggest drought events in Europe from 1950 to 2012. Also according to their results, Northern and Eastern Europe showed the highest drought frequency and severity from the early 1950s to the mid-1970s, while Southern and Western Europe (in particular the Mediterranean area) show the highest drought frequency and severity from the early 1990s onwards.

Accurate estimation of soil moisture conditions is a precursor to formulate better water and land use management practices and hazards mitigation strategies and subsequently ranks high on the priority for food security monitoring (Mishra et al., 2017). Various soil moisture data-based indices have been developed. For example, the Soil Moisture Index (Hunt et al., 2009; Carrão et al., 2016a) is a simple index that normalizes the soil moisture deviation from the mean, taking into account the field capacity and wilting point soil moisture. Modified soil water deficit index (Yang et al., 2017) is an observation data-based index developed as a drought index on the basis of the soil moisture calculated with a crop growth model. Root-weighted soil moisture index (Zhou et al., 2017) accounts for the root-weighted soil water status making a more precise soil moisture state estimation that also accounts for irrigation scheduling, plant growth and yield and water consumption.

Nonetheless, due to the lack of dense ground-based soil moisture measurements data and the difficulties to extrapolate them spatially, alternative ways of characterizing soil moisture drought state have been developed. The most common approach uses drought indices derived from climate variables (Sims et al., 2002; Dai et al., 2004; Mika et al., 2005), while other approaches consider remote sensing measurements and model simulations (Sivakumar et al., 2011). Several tools and indices have been developed to this direction. As an example, soil water deficit index and evapotranspiration deficit index were developed by Narasimhan and Srinivasan (2005), to monitor agricultural drought based on weekly soil moisture and evapotranspiration values simulated by the Soil & Water Assessment Tool (SWAT) hydrologic model. Similarly, Sheffield (2004) use high-resolution, land surface hydrology simulations of Variable Infiltration Capacity (VIC) model to estimate a hydrologically based drought index. Empirical Standardized Soil Moisture Index (Carrão et al., 2016b) is a remote sensing based index designed to classify soil moisture anomalies satellite derived surface moisture data into categories of agricultural drought intensity.

Hydrological (HMs) and Land surface models (LSMs) are indispensable tools for simulating the hydrological status in local to regional and global scale applications. Hydrological models are mainly resolving the hydrological cycle, while land surface schemes are also resolving the energy balance of the land surface. A wealth of studies have compared results of various models in global scale in terms of evaluation of mean and extreme runoff and for their ability to robustly capture climate change impacts (Sood and Smakhtin, 2015; Zhao et al., 2017; Julien et al., 2018; Zaherpour et al., 2018). Regarding the validity of both types of models to capture future drought conditions, Berg et al. (2017), showed that hydrological models intrinsically overestimate future increase in droughts. This happens mainly because they do not account for CO_2 sensitive processes as LSMs do, and hence they cannot simulate reduced plant stomatal conductance under increased atmospheric CO_2 (Milly and Dunne, 2016) that reduce PET (Van den Hoof et al., 2011, 2013) and hence soil moisture depletion. This mechanism has been found to result in more modest climate change impact on evapotranspiration comparing to pure hydrological models (Betts et al., 2018; Koutroulis et al., 2018a). In the recent years, the Inter-Sectoral Impact Model Intercomparison project (ISIMIP) has been introduced to offer a consistent framework for projecting impacts of climate change across various affected sectors and spatial scales, with water sector to be a basic pillar of the project.

Calibration and validation of hydrological and land surface models is usually performed towards their ability to capture discharge (Beven, 1989). Discharge is the most widespread evaluation methodology for a number of reasons, with the most important to be the availability of long term time series of data. Also important is that the discharge of a specific point is the hydrological outcome of an entire upstream area, hence the evaluation of a single point represents the average ability of

the model to approximate a whole area hydrology (Jian et al., 2017). Last but not least, discharge is one of the most important hydrological budget variables. In contrast to the discharge, evaluation of the simulated soil moisture is difficult, due to its distributed character, the luck of long term measurements and the difficulty to remotely sense the soil moisture in depths greater than few centimeters. Nonetheless, many studies have validated hydrological/land surface models towards the available soil moisture data, either from in-situ measurements or remote sensed proxies.

In this research, the evolution of soil moisture droughts in Europe is studied using the Soil Moisture Index (SMI). This index was chosen among others for its simplicity, ease in the interpretation and most importantly due to its estimation on soil moisture data. Climate data projections available by ISIMIP were used to force Joint UK Land Environment Simulator (JULES) land surface model to provide projections of future soil moisture under different climate change scenarios. These JULES runs also contribute to the second phase of the ISIMIP project (ISIMIP2b) as JULES-W1 (W1 suffix is used in the framework of ISIMIP2b to discriminate the specific model setup from other JULES contributions).

This work is organized as follows: In Section 2, the methods that were used are described, i.e. the description of JULES model, the climate model data and scenarios analyzed, the estimation of soil moisture index and the methodology followed to identify drought events in space and time. In Section 3, the results of this study are presented. First, the SMI changes under two different emission scenarios are analyzed for each European region. Second, the change in the occurrence of identified drought events characterized by “severe” and “extreme” SMI values are analyzed. Finally, the findings are discussed and compared to previous studies.

2. Methods

2.1. The JULES land surface model

JULES is being used as a standalone application, but also consists the land surface simulation part of the UK met office numerical atmospheric Model (Walters et al., 2017). JULES comprised of two main parts. The first is the Met Office Surface Exchange Scheme (MOSES; Cox et al., 1998) that is the energy and water balance part of JULES. The second is the Top-down Representation of Interactive Foliage and Flora Including Dynamics (TRIFFID; Cox, 2001) component which is the a dynamic global vegetation model (Cox, 2001; Clark et al., 2010; Best et al., 2011b). The JULES main physics modules are the surface exchange of energy fluxes module, the snow cover module, surface hydrology, soil moisture and temperature, plant physiology, soil carbon and vegetation dynamics module (Best et al., 2011a, 2011b).

In JULES, calculations are being performed in grid cells, that are represented by different surface types. JULES considers nine different land surface types (Best et al., 2011a; Clark et al., 2011), five for vegetation (broadleaf trees, needle leaf trees, (temperate) grasses, (tropical) grasses and shrubs) and four non-vegetated types (urban, inland water, bare soil and ice).

The received precipitation is divided into rainfall and snowfall based on a 274 K temperature threshold (Best et al., 2011a). The runoff is governed by two processes, the surface runoff that follows an infiltration excess mechanism, and sub-surface runoff and drainage through the bottom of the soil column (Best et al., 2011a). The estimation of potential evaporation is performed using the Penman–Monteith method (Penman, 1948).

Soil processes include soil moisture extraction by vegetation, soil thermodynamics and water fluxes. Four soil layers of thicknesses 0.1, 0.25, 0.65 and 2.00 m were used, following the default Global Land configuration, as this setup has been found to capture the soil temperature variations (Best et al., 2011a). The water that reaches the soil splits into water that infiltrates the soil and the surface runoff. The infiltration occurs at a rate equal to the saturated hydraulic conductivity multiplied by correction factor that accounts for the presence and type of vegetation. If a soil layer becomes supersaturated (moisture exceeding field capacity), the water in excess of saturation is put into the layer below. Any excess from the bottom layer becomes subsurface runoff (Best et al. (2011a, 2011b); Clark et al. (2011)). The simulated vegetation access to moisture at each level of the soil is determined by root density and is assumed to follow an exponential distribution with depth (Best et al., 2011a). Hydraulic conductivity characteristics are determined by the relationships of Van Genuchten (1980), that are considered complex but more scientifically robust formulae. Details about the respective equations and the parameter values are provided in Best et al. (2011a). Finally, the JULES leaf stomatal conductance mechanism is described in Jacobs (1994) and Cox et al. (1998).

JULES model is one of the most evaluated land surface model. Its ability to capture soil moisture has been validated in different studies. It has been evaluated for different simulated processes against observed and proxy data, such as photosynthesis related processes (Pacifico et al., 2011), water vapor transfer (Garcia Gonzalez et al., 2012), permafrost simulation (Chadburn et al., 2015), hydrological processes (Gudmundsson et al., 2012; MacKellar et al., 2013; Papadimitriou et al., 2016, 2017; Koutroulis et al., 2018c) and gross primary productivity (Slevin et al., 2014). JULES ability to simulate soil moisture has been discussed in a number of studies. Unnikrishnan et al. (2016) used in-situ observations of soil moisture to validate the UK Met Office modeled soil moisture over India. Their results indicate a good correlation, especially in regions with bare soil, shrubs and regions of agricultural crop. Yee et al. (2013) inter-compare in-situ and satellite data with soil moisture simulated with JULES, in Australia, finding significant correlation between in-situ measurements, satellite soil moisture products and model simulations. Williams and Quaife (2016) compared JULES soil moisture over UK to satellite-derived measurements. They found that the model simulated temporal and spatial patterns reasonably well. Furthermore, JULES correctly simulated the seasonal cycle and correctly identifies the large-scale spatial patterns of soil moisture. Kong et al. (2011) compared MOSES simulated soil moisture to field measurements from an agricultural site of UK, revealing a good agreement.

As mentioned before, JULES uses 4 soil layers, reaching to as deep as 3 m. However, this depth is too deep to affect the agricultural production. The vast majority of the root zone of the five most widely grown crops in the world (wheat, rice, maize, soybeans and barley (Lobell and Field, 2007) does no surpass the one meter in depth, with the 50% to exist shallower than 0.15 m (Hoad et al., 2001; Fan et al., 2016). Hence, the first one meter of depth was considered, by summing the three uppermost layers of soil moisture from the model results.

2.2. Global climate models data

The JULES-W1 model was run with forcings from four Global Climate Models (GCMs) of the fifth phase of the Coupled Model Intercomparison Project (CMIP5) that contribute to the ISIMIP2b experiment, GFDL-ESM2M (Dunne et al., 2012), HADGEM2-ES (Jones et al., 2011), IPSL-CM5A-LR (Dufresne et al., 2013), MIROC5 (Watanabe et al., 2010). These GCMs provided the forcing data in the ISIMIP2b experiment. From the four used GCMs, IPSL-CM5A-LR and HadGEM2-ES are the most sensitive models to changes in the emissions, while MIROC5 and GFLD-ESM2M have been found to be less sensitive (Warszawski et al., 2014; Julien et al., 2018). Discussion about the model selection and the ISIMIP2b experiment is found in Frieler et al. (2017). McSweeney and Jones (2016) analyzed the representativeness of these GCMs (plus one that was left out later from ISIMIP) comparing to the entire 36 GCM ensemble of CMIP5 experiment. Discussion about the ability of the GCMs to reproduce observed precipitation and temperature can be found in Koutroulis et al. (2016). The GCM data were provided bias corrected using EartH2Observe observations, WFDEI and ERA-Interim data Merged and Bias-corrected for ISIMIP (EWEMBI) dataset (Lange,

2016, 2017), as an essential pre-processing step before being used in climate change impacts assessment (Grillakis et al., 2017; Papadimitriou et al., 2017).

Three different experiments data were used, the historical period experiment, with historical CO_2 emissions to increase from 1850 (286 ppm CO_2) to 2005 (379 ppm CO_2). Beyond 2005, two Representative Concentration Pathway (RCPs) scenarios were considered. The first is the low emission RCP 2.6 scenario. This scenario is described as the best case for limiting anthropogenic climate change and assumes aggressive mitigation measures application. In this scenario, the CO_2 emissions are peaking in the 2020s at around 440 ppm, with a slow decline to follow to as far as 2100. The second scenario is RCP 6.0, described as a medium-high RCP with stabilization from 2150 onwards. In this scenario, emissions peak by 2060 and then decrease drastically, but remain well above the current levels. In this scenario, the CO_2 concentration continues rising at a slower rate in the latter parts of the century, reaching 620 ppm by 2100 (Van Vuuren et al., 2011).

JULES-W1 model utilizes a number of GCM land surface variables, specifically, maximum, minimum and mean daily temperature, shortwave and longwave downwelling radiation, surface wind speed, specific humidity, precipitation and surface pressure. JULES-W1 is run in sub-daily time step, and in a spatial resolution of 0.5°. Both bias corrected GCM land surface variables and JULES output data (including soil moisture for different depths) are available from ISIMIP under the ISIMIP terms of use. The JULES science configuration used in this study was based on the Global Land configuration version 4 (GL4.0 - Walters et al., 2014). This configuration uses soil data from the Harmonized World Soil Database (Nachtergaele et al., 2008) and land use parameters of Global Soil Data Task database (IGBP-DIS, 2000).

2.3. Soil moisture index

Soil Moisture Index (Hunt et al., 2009) uses soil water measurements, normalized between known field capacity and wilting point. To estimate the SMI, the fraction of the available water (F_{AW}) is obtained by Eq. 1, where θ is the volumetric soil water content, θ_{WP} is the wilting point soil water and θ_{FC} is the field capacity. F_{AW} varies between 0 and 1 for wilting point and field capacity soil water conditions respectively. In his work Baier (1969) correlated F_{AW} to ET, indicating that for F_{AW} values beyond 0.5, the ET does not vary, while below that value, it reduces linearly. From F_{AW}, the SMI is scaled between −5 and 5 using Eq. (2). By design, when F_{AW} equals 0.5, SMI is 0, and hence at this value the stressing conditions in terms of ET are separated to the optimal ET conditions (Hunt et al., 2009).

$$F_{AW} = \frac{\theta - \theta_{WP}}{\theta_{FC} - \theta_{WP}} \quad (1)$$

$$SMI = -5 + 10F_{AW} \quad (2)$$

The estimated SMI index is then characterized according to Table 1 for its negative values, with drought conditions to intensify as SMI decreases from 0 (Sridhar et al., 2008).

Additionally, a modification was applied to the SMI in order to remove the inherent seasonality of soil moisture and make SMI values comparable across different seasons. The modification uses the long term monthly minimum and maximum soil moisture content instead of θ_{WP} and θ_{FC}. A similar approach was employed by Narasimhan and Srinivasan (2005) to formulate the Soil Moisture Deficit Index (SMDI). The long term monthly minimum and maximum soil moisture content,was considered for both the historical and the as well as both scenario projection data from each GCM. This type of normalization that uses the minimum and maximum records instead of θ_{WP} and θ_{FC} has also been used to estimate SMI on remote sensing data in Zhang et al. (2017).

Table 1
SMI drought states.

Drought condition	SMI range
Less intense	>0 to ≤−1
Moderate	≥1 to ≤−2
High	≥2 to ≤−3
Severe	≥3 to ≤−4
Extreme	≥4 to ≤−5

2.4. Soil moisture drought identification in the space and time

There are two major characteristics to describe a drought (Yevjevich, 1967; Mishra and Singh, 2010). The first characteristic is the duration, which is the time between the start and the end of drought state, defined as passing a threshold on a drought related index or quantity. The duration is usually expressed in months (e.g. Koutroulis et al., 2011; Wang et al., 2011; Spinoni et al., 2015). The second characteristic is the intensity of the drought, which is the degree to which the specific drought threshold is exceeded in the drought related index of quantity units. The time integral of the drought intensity between the start and the finish of the drought event gives the severity of the event. This implies that drought events of different intensity can result in similar severity, due to the different duration of each event. Both drought types may have significant negative impacts, however the more intense can be more disastrous due to their acuteness and the inherent inertia of the human systems that impede adaptation measures. An additional important aspect of the drought events is the affected area. Here, spatially and temporally contiguous regions where SMI is below a predefined threshold are identified as a single drought event. A drought event may start on a specific time, affecting a specific area with a spatially varying intensity. As time evolves, the intensity may become more severe or mild, as well the affected area may also change. Despite the evolution of the phenomenon, the drought event can be considered as being a single event caused by the same climatic drivers, e.g. by a resilient high pressure system present over a region for several months, as it is the case of the 2018 European drought in the central – northern Europe. In order to avoid connecting two different drought events with tenuous spatial connectivity, a threshold for area was also applied. Typically used thresholds range between 25,000 and 150,000 km^2 (Wang et al., 2011). In this study, the threshold was set at 50,000 km^2. Additional restriction was used in the duration of the identified events. Usually agriculture related drought phenomena are studied in temporal scales beyond 12 months (Koutroulis et al., 2011). However, in Mediterranean regions where the precipitation is highly seasonal and occurs in winter months, a drought in the rain season affects the entire year. Hence, a smaller threshold of 7 months of duration was chosen. Furthermore, the threshold for SMI was set at below −3 which corresponds to the “severe” and “extreme” soil moisture drought categories of the index. A visual representation of two drought events evolving in space and time is provided in Fig. 1. Vertical axis represents the time in months, while the color scale depicts the evolution in the SMI (below −3) for each time step. A spatial resolution of 0.5° and monthly time step were used as a basis of the analysis, following the soil moisture data resolutions.

2.5. Case study area

The drought analysis was focused in the European domain with explicit analysis in the different European sub-regions (Fig. 2). The clustering to different sub-regions follows the PRUDENCE project analysis, which has been also used for impact analysis in the recent study of Jacob et al. (2018a, 2018b).

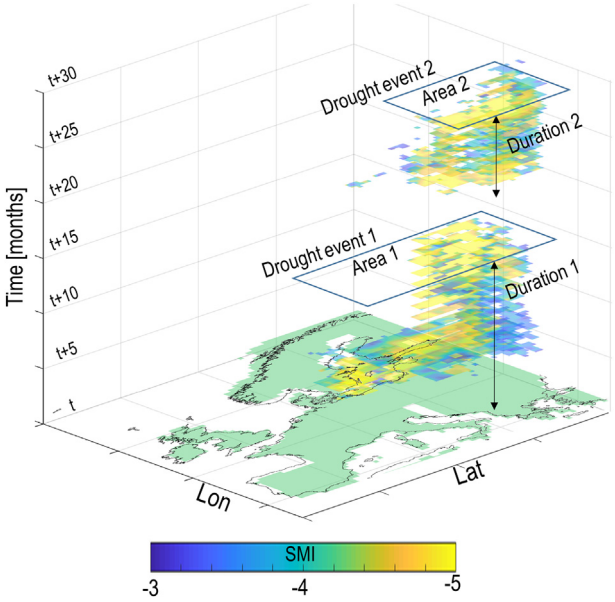

Fig. 1. Identification of two drought events evolving in space and time domains.

3. Results

3.1. Future trends of SMI under climate change

Based on the analysis of the multi-GCM ensemble, Fig. 3 shows the fraction of the area of each focus region that exhibits SMI drought under the RCP 2.6 scenario. The peak and decline pattern of the radiative forcing is also visible in the SMI which in most of the regions show a stabilization after 2030's. In this scenario, drought areas characterized as *less intense* are shown to be rather constant or even slightly decrease. *Moderate* drought affected areas are also exhibiting slight changes, with the most noteworthy to be a slight gradual decrease in Mediterranean and a slight increase in Mid-Europe, France and Scandinavia. Areas in the *High* SMI category are expected to increase and stabilize in France, Mid-Europe, Scandinavia, Eastern Europe and British Isles. In the rest of the regions, changes are projected more mild for this category. *Severe* SMI category is shown to increase and stabilize for all regions, with Eastern Europe, Mediterranean and Eastern Mediterranean to exhibit the larger changes. *Extreme* drought regions are expected to increase and stabilize for most of the regions, however, it is shown that other are expected to face gradual increase to as far as the end of the century. These are the Mediterranean region, Eastern Europe, and Eastern Mediterranean. Beyond the analysis of the future trends, important is the projected change of SMI within the negative index space in the future. To assess this, three periods were selected out of the transient run. These are the historical 1966–2005, the near future (NF) 2020–2059 and the far future (FF) 2060–2099. This methodology has been widely used in climate change impact studies (Daliakopoulos et al., 2017) as it provides a concise comparison of the impact in a future period comparing to the similar length past period. The periods were chosen to consider the modeled historical period and forthcoming future periods, excluding the almost already lapsed 2006–2019 years. The changes in the NF and FF are estimated relatively to the historical results are summarized in Table 2. Overall, the most pronounced changes in terms of percent increase of the area experiencing negative SMI values are projected for the near future (2020–2059) for Eastern Europe (16.6%), Mid Europe (11.8%) and Scandinavia (11.4%). The respective most affected regions for the far future (2060–2099) are Eastern Europe (18.6%), Mediterranean (14.1%) and Eastern Mediterranean (12.2%).

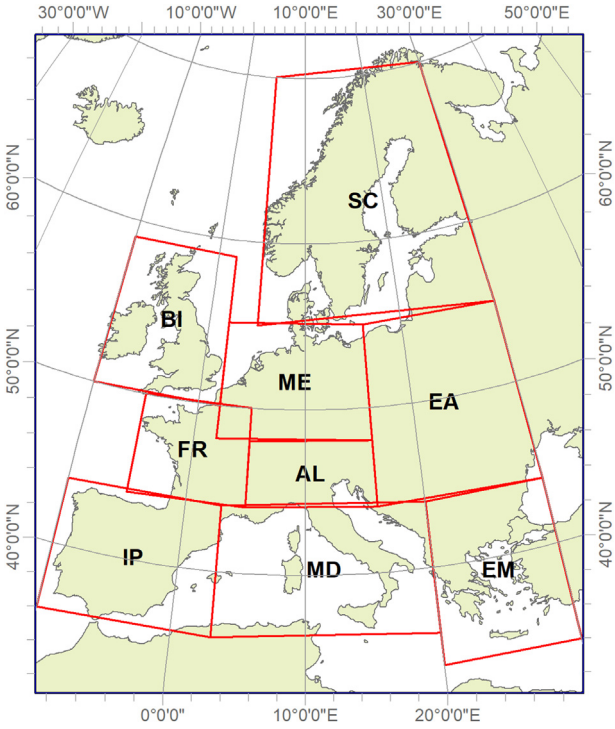

Fig. 2. Case study area and analysis regions: BI = British Isles, FR = France, IP = Iberian Peninsula, MD = Mediterranean, AL = Alps, ME = Mid-Europe, EA = Eastern Europe, EM = East Mediterranean (regions based on (Christensen and Christensen, 2007)-modified).

For the medium-high scenario RCP 6.0, the changes in the *Less Intense* and *Moderate* SMI drought categories are expected to be similar to the RCP 2.6 scenario, or even milder in some cases in the near future period (Iberian Peninsula, France, Mediterranean, Eastern Europe). The percentage of area under *High* and *Severe* SMI category is expected to be similar to the RCP 2.6 until the mid of the century and then is expected to increase for almost all regions, except Iberian Peninsula that is expected to decline. Nonetheless, this recession in the fraction of the area under *High* and *Severe* SMI drought at the end of the century is due to the strong increase in the *Extreme* drought. Strong increase in the *Extreme* SMI drought affected area is also simulated in the second half of the century for France, Mediterranean, Alps, Eastern Mediterranean and Eastern Europe (Fig. 4). The changes in the NF and FF also for this scenario are summarized in Table 2. Summarizing, the largest increase in the area experiencing negative SMI values are projected in the near future for Eastern Europe (11.4%), Mediterranean (11.6%), Scandinavia (9.1%) and Mediterranean (9.2%). The respective most affected regions in the far future period are Eastern Europe (21.4%), Mid-Europe (19.1%) and France (18%).

3.2. Changes in the severe and extreme soil moisture droughts

Beyond the analysis in the regional trends of change in SMI, a more important aspect that is addressed here is how significant drought event episodes' characteristics are expected to change in the future. The drought event analysis was performed on the SMI less than −3 (severe and extreme classes). Discrete drought events were identified in the space and time following the methodology described in Section 2.4. Average area of the drought, its duration and intensity, as well as the time of occurrence event of each drought were identified. Results are presented in Fig. 5 and Table 3. The historical period droughts (as simulated by all model runs) are presented in red, while the size of the blobs indicate the duration of the drought. Considering events that affect area larger than 10^6 km^2 (that is twice the size of Spain), there is only one such event in the historical simulations (simulated by HadGEM3) with a simulated duration of 11 months. For the RCP 2.6, there are limited area drought events of intensity beyond the most severe simulated in the historical period (average SMI < −4.4), as well

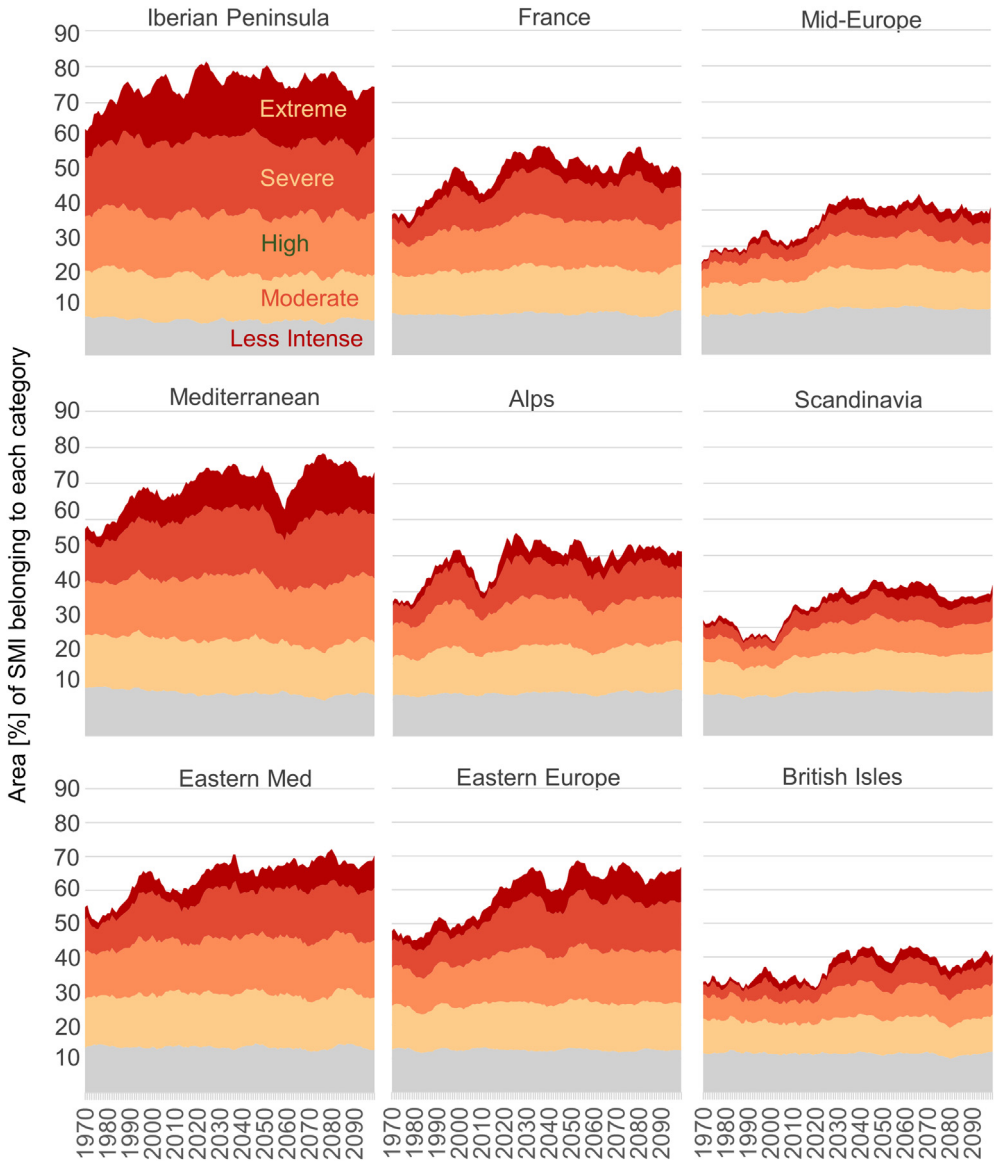

Fig. 3. Percent of area within each SMI drought category for the focus regions, under RCP 2.6 scenario. Timeseries smoothed by a ten-years moving average.

as events that affect areas much larger than those in the historical period (Fig. 5). In the near future, RCP 2.6 simulations project a 27% increase in the number of drought events, with a 16% increase in the mean duration and a 46% increase in the mean occupied area. The respective increase in the far future period is 115% in the number of events, 30% in the duration and 15% in the area. Regarding the events larger than 10^6 km^2, the near future simulations project a eleven-fold increase with a 59% increase in the duration, while for the far future the increase is projected to 14-fold with an increase in the duration of 187% (Table 3). Individual events that emerge after the mid of the 21st century are simulated to reach up to 7 years in duration (Fig. 5). On the other hand, while RCP 6.0 simulations show smaller increase in the number of drought events in the near future (22%), substantially smaller increase in the average occupied area (23%), but larger increase in the duration (19%). The respective increase in the far future period is 123% in the number of events, and 26% in the area and a significant larger increase in the average duration (48%). Furthermore, for the events that affect area larger than 10^6 Km^2 the changes are projected to be milder than RCP 2.6 in the near future (7-fold in the event number) but with larger duration (85% increase). Nonetheless in the far future, the increase in the occurrence is projected to be 28-fold and 246% in the duration.

Fig. 6a shows the spatial distribution of severe and extreme SMI drought (in years) in the historical (1966–2005) period simulations (average of the four GCM runs). It is found that the most prone areas are the south Iberian and the near Black Sea Eastern Mediterranean and Eastern Europe regions, with more than ten and eight years respectively in severe drought or extreme drought conditions in the 40 year period. The near future RCP 2.6 simulations (Fig. 6b) show the largest increase in the severe and extreme drought, with the eastern Europe and Eastern Mediterranean to expect 4–6 years or even more additional severe or extreme drought conditions between 2020 and 2059. In contrast, RCP 6.0 (Fig. 6c) project less change with only an increase between 3 and 5 years at the western - coastal Black sea regions,. A decrease in the total duration of drought is observed in the western Iberian. For the far future and RCP 2.6, patterns for eastern Europe are similar to the near future but with a stronger increase signal between 5 and 6 year in the respective 40 year period (Fig. 6d). Also Greece, Sardinia and south Iberian are expected to have an increase in severe or extreme drought conditions of >5 years. Again here, western Iberian is simulated

Table 2
Change in the area fraction for each negative SMI category, for near future (2020–2059) and far future (2060–2099) and for the two radiative forcing scenarios, RCP 2.6 and RCP 6.0.

		2020-2059						2060-2099					
		Extreme	Severe	High	Moderate	Less intens	Sum	Extreme	Severe	High	Moderate	Less intens	Sum
RCP 2.6	Iberian Peninsula	4.1	1.7	0.4	-0.5	-0.6	5.1	3.4	1.0	0.3	-0.3	-0.4	4.0
	France	2.0	3.4	3.0	1.5	0.6	10.4	2.0	2.6	2.1	1.2	0.5	8.3
	Mid-Europe	2.2	3.1	2.8	2.2	1.4	11.8	2.5	2.7	2.4	1.9	1.3	10.8
	Scandinavia	2.1	3.1	2.8	2.1	1.3	11.4	2.1	3.0	2.5	1.8	1.0	10.4
	Alps	2.6	2.2	1.7	1.1	0.6	8.1	2.2	1.9	1.3	1.3	1.1	7.8
	Mediterranean	4.4	3.8	2.1	0.3	-1.0	9.6	8.0	5.7	2.2	-0.1	-1.7	14.1
	Eastern Europe	4.6	5.8	4.2	1.9	0.1	16.6	6.5	6.4	4.2	1.8	-0.3	18.6
	British Isles	1.3	2.8	2.7	1.2	0.0	7.9	0.7	2.2	2.1	1.0	-0.1	5.8
	Eastern Mediterranean	3.5	3.3	2.0	0.8	0.0	9.6	5.4	4.8	2.1	0.4	-0.3	12.2
RCP 6.0	Iberian Peninsula	2.4	1.3	0.8	0.6	0.4	5.4	11.1	2.6	-0.6	-1.4	-1.6	10.1
	France	0.9	2.4	2.3	1.6	0.6	7.9	6.3	6.3	4.2	1.4	-0.2	18.0
	Mid-Europe	1.2	1.9	2.1	1.9	1.3	8.4	4.4	5.0	4.6	3.4	1.7	19.1
	Scandinavia	1.1	2.2	2.4	2.1	1.3	9.1	3.4	4.0	3.6	2.7	1.3	15.1
	Alps	0.9	0.9	1.0	1.0	0.8	4.6	4.5	4.3	3.0	1.8	0.8	14.3
	Mediterranean	3.9	4.3	3.0	1.0	-0.5	11.6	8.2	6.7	3.0	0.1	-1.8	16.3
	Eastern Europe	2.7	3.4	2.9	1.9	0.5	11.4	7.4	7.7	5.0	2.1	-0.6	21.4
	British Isles	0.8	1.8	1.6	0.7	0.0	4.9	2.2	3.3	2.3	0.9	-0.3	8.2
	Eastern Mediterranean	2.3	2.2	2.1	1.5	0.9	9.2	5.6	4.8	2.8	0.9	-0.4	13.7

to have a decrease in the duration under severe and extreme SMI drought. Finally, for the far future RCP 8.5 projection, results show the largest change, with entire Europe except Alps, Ireland, northern England and northern Norway, to expect significant increase in severe and extreme SMI drought conditions. Southern Iberia, Greece and East Europe are the most affected with increase of severe or extreme drought conditions to as high as 5 to 6 or more years for the 40 year period (Fig. 6e).

4. Discussion

As a consequence of the anticipated changes in the climate, precipitation and evapotranspiration patterns are expected to pose changes to the soil moisture content in European region. Here, two future emission scenarios were analyzed, the RCP2.6 that assumes an aggressive mitigation, peaking the CO_2 emissions in the mid of the century and then decreasing, and a some mitigation scenario that assumes the emissions to rise to as far as the end of the century.

Soil moisture simulations from JULES Land Surface model were used to estimate the Soil Moisture Index, on which the analysis was based. The SMI is a simple but robust index that is found to be widely used in the literature. Its major simplification concerns the assumed correlation between F_{AW} and ET that assume that for F_{AW} values beyond 0.5, the ET does not vary, while below that value, it reduces linearly. A question that raises is whether also in JULES the ET remains constant for F_{AW} values beyond 0.5. Nonetheless, in the present study only drought conditions, i.e. F_{AW} values below 0.5 were studied, while the F_{AW} space below 0.5 is just used for the segmentation of drought characterization into 5 categories. Beyond its limitations, SMI drought assessment has been found to be less sensitive to the projected climate change comparing to PDSI index (Samaniego et al., 2018).

The identified trends of change in the SMI droughts found in this study show a similar to the emission scenarios' storylines changes. This is a peak and decline (or stabilize) pattern for the change in negative SMI values in RCP 2.6, and a continuously increasing respective pattern for SMI under the RCP 6.0. These increasingly drying patterns are in the same direction with the findings of Ruosteenoja et al. (2018) that analyzed future GCM simulated soil moisture of the more aggressive climate change scenario RCP 8.5, but also the drought analysis of Daliakopoulos et al. (2017) on RCP 2.6 and RCP 8.5 scenarios. Consistent and more severe with the foregoing results are the findings of (Berg et al., 2017) that have shown large-scale drying of surface soils in Europe under RCP8.5, as well as (Koutroulis, 2019) who studied the same high-rate RCP 8.5 scenario, indicating notable increase in the aridity over southern European countries. Results also confirm and update the previous findings of a robust signal for water scarcity in Mediterranean region (Koutroulis et al., 2015). Furthermore, according to the research findings of (Orth and Destouni, 2018), the demonstrated impacts on soil moisture resources suggest the even more drastic reduction of blue-water fluxes.

The two studied emission scenarios exhibit similar SMI drought changes in the near future, with the milder RCP 2.6 scenario to exhibit slightly more significant increase. While this seems inconsistent with the general storyline description of the two scenarios, this can be attributed to their near future carbon fluxes description. The considered emissions are found to be higher in the RCP 2.6 between 2005 and 2025, posing more significant changes in the beginning of the near future period (Walsh et al., 2017). On the other hand, RCP 6.0 emissions are relatively stable to as far as 2030s and then increase steadily to 2100.

Exceptionally low soil moisture content that is expected to cause severe or extreme SMI drought conditions is found to become substantially more frequent than recent past, especially in the Iberian Peninsula, eastern Europe and Mediterranean regions. Albeit the receding trend of RCP 2.6 in the second half of the 21st, the event analysis performed here showed severe and extreme droughts are expected to increase in occurrence and duration in the future. As an exception, only the occupying area of each drought event was found to follow the receding emissions pattern of the RCP 2.6 in the end of the century. The RCP 6.0 scenario shows a less aggressive soil moisture droughts increase in the near future, followed by a rapid increase in the far future period. Also, it was found that in the context of the defined severe and extreme drought events, the most prone to change parameter is the

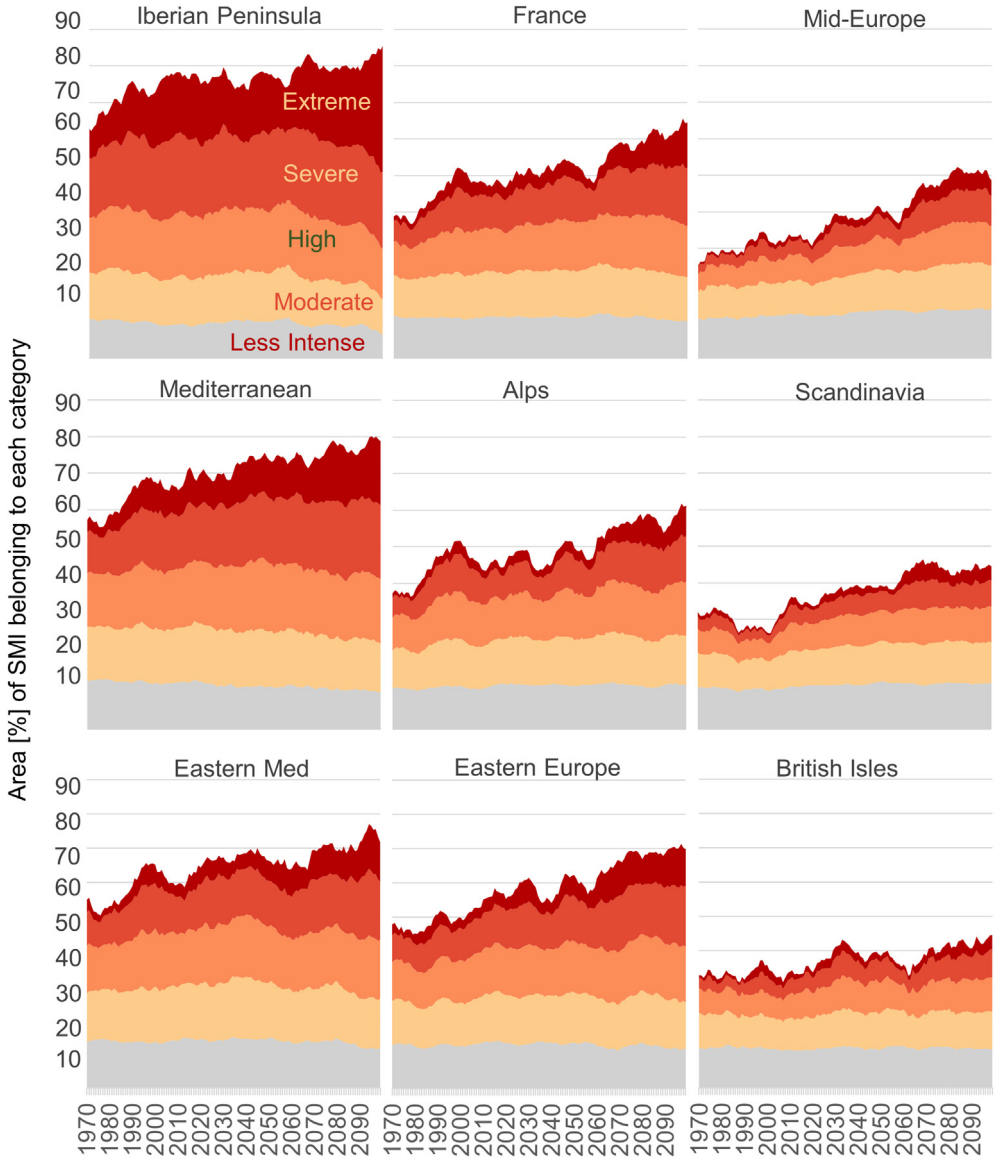

Fig. 4. Percent of area within each SMI drought category for the focus regions, under RCP 6.0 scenario. Timeseries smoothed by a ten-years moving average.

affected area and then the duration. In their work, Samaniego et al. (2018) studied the changes in the extreme drought events in different levels of climate warming. Their results point to the same direction, indicating that Europe is expected to face unprecedented increases in the area affected by the large soil moisture droughts and their duration.

Moreover, results show that unprecedented drought events in the historical period are expected to occur both in the near future as well as to the end of the century and for both scenarios, regardless the degree of mitigation that will be followed. These events are characterized by their unforeseen spatial extent, duration that can reach up to 3 years, but also the increased frequency of occurrence that can reach one or two events per decade.

Attributing the SMI changes to specific climatic variables is a rather daunting task. The change in the soil moisture dynamics and hence the SMI is subject to a complex combination of changes in the climate variables. Temperature increase plays an important role among the parameters that enhance evaporation process, as well as changes in the precipitation. Furthermore, Manning et al. (2018) found that precipitation exerts the main control over droughts in soil moisture, with potential evapotranspiration to play a key role on the onset, the severity and the persistence of the events. Nonetheless, a number of other factors that affect evapotranspiration (wind, radiation) impact the SMI, as well as the CO2 concentrations that affect the leaf transpiration. Moreover, vegetation and the interactions between different vegetation types play a significant role on the soil moisture availability (Van den Hoof and Lambert, 2016). The JULES model incorporates all these mechanisms and provides a concise picture of their combined effect on soil moisture. Manning et al. (2018) emphasizes the oversimplification that climatic water balance relationships (such as *SPE*I and PDSI) assume in the soil moisture drought research, with potential loss of information, or even the inclusion of redundant information in long integration periods of the indices.

The novelty of this work lies on the methodology used for the identification of the drought events in space and time. This methodology, allowed for the analysis of temporarily and spatially consistent drought event characteristics, rather than statistical analysis of the duration, severity and intensity. Another strength of this study is the use of soil moisture data rather than proxy meteorological parameters based indices. The use of land surface model simulations provides the advantage of accounting for the different possible future CO2 concentrations that affect plant transpiration and soil moisture depletion. As a limitation, this analysis is based on the estimation of an index and the application of specific thresholds on it which gives a certain subjectivity to the results. Additionally, no other sources of information that can aid the

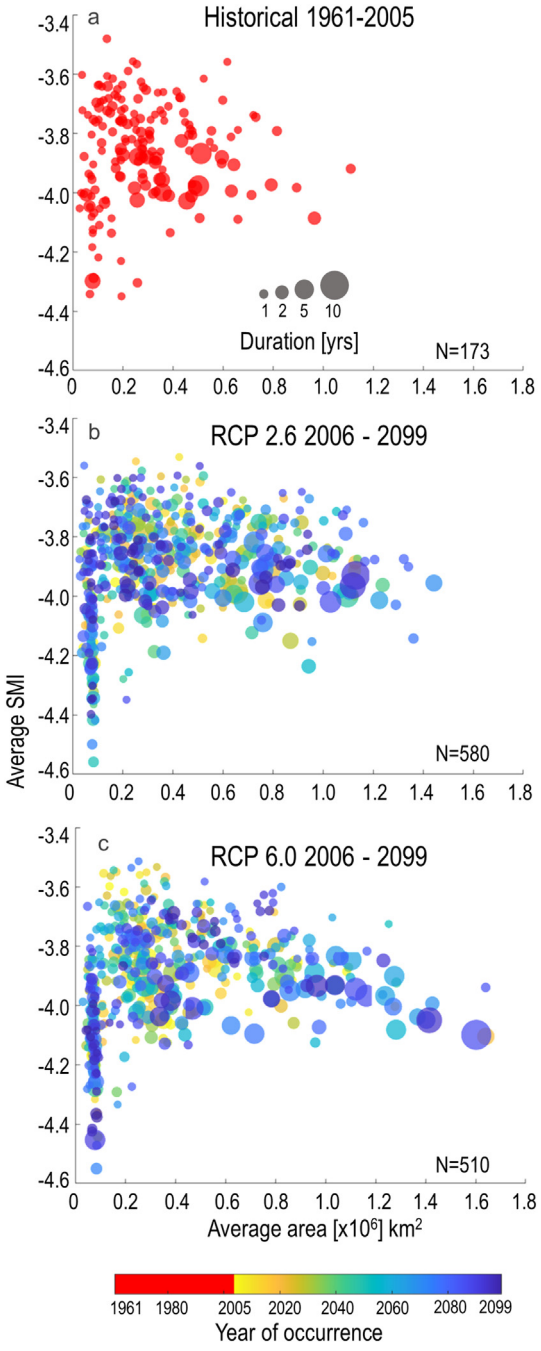

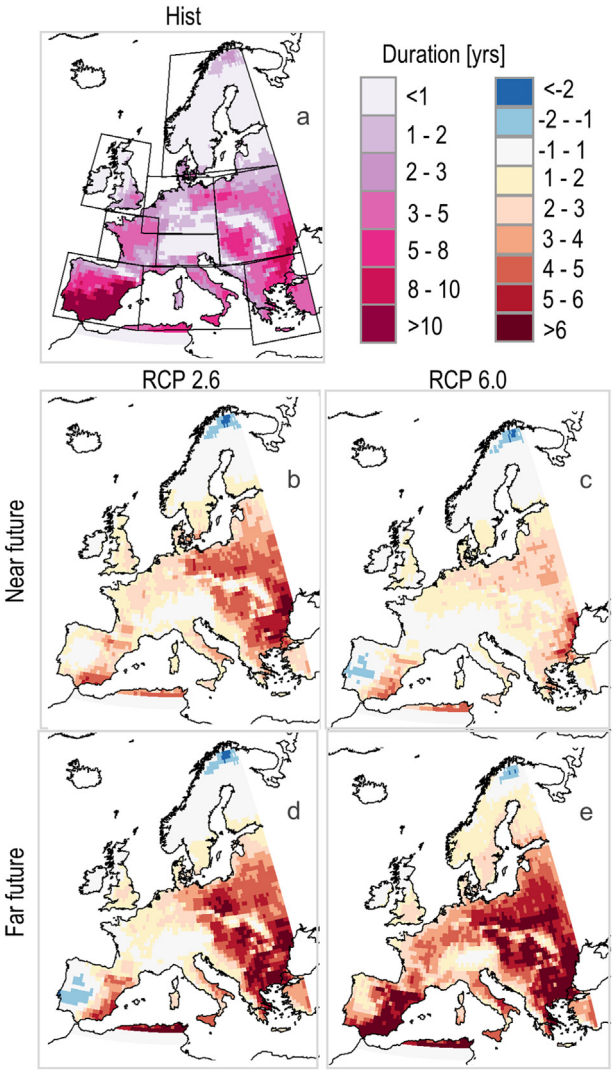

Fig. 5. Identified drought event characteristics. Scatter plots indicate average intensity of the event expressed by the average SMI value versus the average area affected (in millions km^2). Year of occurrence is denoted by the color and the duration by the bubble size.

Fig. 6. Average time of European domain under severe and extreme soil moisture drought in the historical (1966–2006) period (a). Change in duration (in months) for the near future (b, c) and far future (d, e), for the two examined scenarios.

identification and characterization of droughts (e.g. East Atlantic, Azores anticyclone, Northern Annular Mode, downward net radiative fluxes and sea surface temperatures (García-Herrera et al., 2010)).

5. Conclusions

The presented drought analysis provide useful insights for European decision makers to develop informed climate policy. Even following the strong mitigation scenario, governments should be prepared to deal with drought-driven challenges and reduced green water resources.

Table 3
Severe and extreme SMI drought events characteristics for the historical 1961–2005, the near future 2020–2059 and the far future 2060–2099 periods, for RCP 2.6 and RCP 6.0 scenarios. Numbers in the parentheses indicate percent change relatively to the historical period simulations. Results for each GCM are provided in the supplementary material.

	Period	All identified events					Events with area >10^6 Km^2				
		Number of events	Events per year	Mean duration (months)	Average Area (km^2)	Average intensity (SMI)	Number of events	Events per 10 yrs	Mean duration (months)	Average area (km^2)	Average intensity (SMI)
	Historical	40	1.0	10.8	286,781	−3.86	0.3	0.26	11.0	1,109,844	−3.92
RCP 2.6	NF	50 (27%)	1.3	12.5 (16%)	418,001 (46%)	−3.89	3.0 (1100%)	1.24	17.5 (59%)	1,089,809 (−2%)	−3.89
	FF	85 (115%)	2.2	14.0 (30%)	328,197 (14%)	−3.91	3.8 (1400%)	1.73	31.5 (187%)	1,152,687 (4%)	−3.95
RCP 6.0	NF	48 (22%)	1.2	12.8 (19%)	351,343 (23%)	−3.88	2.0 (700%)	0.96	20.4 (85%)	1,255,417 (13%)	−3.95
	FF	88 (123%)	2.3	16.0 (48%)	362,550 (26%)	−3.95	7.3 (2800%)	2.82	38.0 (246%)	1,283,824 (16%)	−3.98

This study found that both studied emission scenarios exhibit similar SMI drought changes in the near future, with the milder RCP 2.6 scenario to exhibit a slightly more significant increase, while the RCP 6.0 to exhibit more significant drought increase in the far future. Furthermore, it was found that severe or extreme droughts are expected to become substantially more frequent than the recent past, especially in the Iberian Peninsula, eastern Europe and Mediterranean regions. Finally, a significant conclusion of the study was that unprecedented drought events in the historical period are expected to occur both in the near future as well as to the end of the century according to both the studied scenarios, i.e. regardless the degree of mitigation that will be followed.

This study therefore urges the need of adaptation to increased drought risk in Europe and especially in Iberian Peninsula, eastern Europe and Mediterranean regions. Especially vulnerable sectors such as agriculture should adapt to the more frequent occurrences of reduced soil water resources. Potential adaptation measurements found in the literature that can mitigate the soil moisture drought impact may include cultivation of different varieties of wheat and maize (Webber et al., 2018). Moreover, mixing of plant functional types that has been found to improve the resistance of the ecosystem, that has been found to mitigating the negative effect of mild and extreme drought events (Van den Hoof and Lambert, 2016). This research improves our understanding on the impacts of climate change on soil water resources, aiding the solutions towards the Sustainable Development related with food and water security/resources and climate change.

Supplementary data to this article can be found online at https://doi.org/10.1016/j.scitotenv.2019.01.001.

References

Baier, W., 1969. Concepts of soil moisture availability and their effect on soil moisture estimates from a meteorological budget. Agric. Meteorol. 6, 165–178. https://doi.org/10.1016/0002-1571(69)90002-8.

Berg, A., Sheffield, J., Milly, P.C.D., 2017. Divergent surface and total soil moisture projections under global warming. Geophys. Res. Lett. 44, 236–244. https://doi.org/10.1002/2016GL071921.

Best, M.J., Pryor, M., Clark, D.B., et al., 2011a. The joint UK land environment simulator (JULES), model description – part 1: energy and water fluxes. Geosci. Model Dev. 4, 677–699. https://doi.org/10.5194/gmd-4-677-2011.

Best, M.J., Pryor, M., Clark, D.B., et al., 2011b. Geoscientific model development the joint UK land environment simulator (JULES), model description – part 1: energy and water fluxes. Geosci. Model Dev. 4, 677–699. https://doi.org/10.5194/gmd-4-677-2011.

Betts, R.A., Alfieri, L., Bradshaw, C., et al., 2018. Changes in climate extremes, fresh water availability and vulnerability to food insecurity projected at 1.5 °C and 2 °C global warming with a higher-resolution global climate model. Phil. Trans. R. Soc. A 376, 20160452. https://doi.org/10.1098/RSTA.2016.0452.

Beven, K., 1989. Changing ideas in hydrology—the case of physically-based models. J. Hydrol. 105 (1-2), 157–172.

Carrão, H., Russo, S., Sepulcre-Canto, G., Barbosa, P., 2016a. An empirical standardized soil moisture index for agricultural drought assessment from remotely sensed data. Int. J. Appl. Earth Obs. Geoinf. 48, 74–84. https://doi.org/10.1016/J.JAG.2015.06.011.

Carrão, H., Russo, S., Sepulcre-Canto, G., Barbosa, P., 2016b. An empirical standardized soil moisture index for agricultural drought assessment from remotely sensed data. Int. J. Appl. Earth Obs. Geoinf. 48, 74–84. https://doi.org/10.1016/J.JAG.2015.06.011.

Chadburn, S., Burke, E., Essery, R., et al., 2015. An improved representation of physical permafrost dynamics in the JULES land-surface model. Geosci. Model Dev. 8, 1493–1508. https://doi.org/10.5194/gmd-8-1493-2015.

Christensen, H.J., Christensen, B.O., 2007. A summary of the PRUDENCE model projections of changes in European climate by the end of this century. Clim. Res. 81, 7–30. https://doi.org/10.1007/s10584-006-9210-7.

Ciais, P., Reichstein, M., Viovy, N., et al., 2005. Europe-wide reduction in primary productivity caused by the heat and drought in 2003. Nature 437, 529–533. https://doi.org/10.1038/nature03972.

Clark, D., Harris, P., Pryor, M., Hendry, M., 2010. Joint UK Land Environment Simulator (JULES) Version 2.2 User Manual.

Clark, D.B., Mercado, L.M., Sitch, S., et al., 2011. The joint UK land environment simulator (JULES), model description – part 2: carbon fluxes and vegetation dynamics. Geosci. Model Dev. 4, 701–722. https://doi.org/10.5194/gmd-4-701-2011.

Cox, P.M., 2001. Description of the "TRIFFID" dynamic global vegetation model. Hadley Cent Tech Note. 24, pp. 1–17.

Cox, P., Huntingford, C., Harding, R., 1998. A canopy conductance and photosynthesis model for use in a GCM land surface scheme. J. Hydrol. 212–213, 79–94. https://doi.org/10.1016/S0022-1694(98)00203-0.

Dai, A., Trenberth, K.E., Qian, T., 2004. A global dataset of palmer drought severity index for 1870–2002: relationship with soil moisture and effects of surface warming. J. Hydrometeorol. 5, 1117–1130. https://doi.org/10.1175/JHM-386.1.

Daliakopoulos, I.N., Pappa, P., Grillakis, M.G., et al., 2016. Modeling soil salinity in greenhouse cultivations under a changing climate with SALTMED. Soil Sci. 181, 241–251. https://doi.org/10.1097/SS.0000000000000161.

Daliakopoulos, I.N., Panagea, I.S., Tsanis, I.K., et al., 2017. Yield response of Mediterranean rangelands under a changing climate. Land Degrad. Dev. https://doi.org/10.1002/ldr.2717.

Dufresne, J.-L., Foujols, M.-A., Denvil, S., et al., 2013. Climate change projections using the IPSL-CM5 Earth system model: from CMIP3 to CMIP5. Clim. Dyn. 40, 2123–2165. https://doi.org/10.1007/s00382-012-1636-1.

Dunne, J.P., John, J.G., Adcroft, A.J., et al., 2012. GFDL's ESM2 global coupled climate–carbon earth system models. Part I: physical formulation and baseline simulation characteristics. J. Clim. 25, 6646–6665. https://doi.org/10.1175/JCLI-D-11-00560.1.

Euractiv, 2018. Extreme drought causes EU vegetables 'most serious' crisis in 40 years – EURACTIV.com. Euractiv https://www.euractiv.com/section/agriculture-food/news/extreme-drought-causes-eu-vegetables-most-serious-crisis-in-40-years/ (Accessed 14 Sep 2018).

Fan, J., McConkey, B., Wang, H., Janzen, H., 2016. Root distribution by depth for temperate agricultural crops. Field Crop Res. 189, 68–74. https://doi.org/10.1016/J.FCR.2016.02.013.

Frieler, K., Lange, S., Piontek, F., et al., 2017. Assessing the impacts of 1.5 °C global warming – simulation protocol of the inter-sectoral impact model Intercomparison project (ISIMIP2b). Geosci. Model Dev. 10, 4321–4345. https://doi.org/10.5194/gmd-10-4321-2017.

Garcia Gonzalez, R., Verhoef, A., Luigi Vidale, P., Braud, I., 2012. Incorporation of water vapor transfer in the JULES land surface model: implications for key soil variables and land surface fluxes. Water Resour. Res. 48. https://doi.org/10.1029/2011WR011811 (n/a-n/a).

García-Herrera, R., Díaz, J., Trigo, R.M., et al., 2010. A review of the European summer heat wave of 2003. Crit. Rev. Environ. Sci. Technol. 40, 267–306. https://doi.org/10.1080/10643380802238137.

Ghannam, K., Nakai, T., Paschalis, A., et al., 2016. Persistence and memory timescales in root-zone soil moisture dynamics. Water Resour. Res. 52, 1427–1445. https://doi.org/10.1002/2015WR017983.

Grillakis, M.G., Koutroulis, A.G., Komma, J., et al., 2016a. Initial soil moisture effects on flash flood generation - a comparison between basins of contrasting hydro-climatic conditions. J. Hydrol. https://doi.org/10.1016/j.jhydrol.2016.03.007.

Grillakis, M.G., Koutroulis, A.G., Tsanis, I.K., 2016b. The 2 °C global warming effect on summer European tourism through different indices. Int. J. Biometeorol. https://doi.org/10.1007/s00484-015-1115-6.

Grillakis, M.G., Koutroulis, A.G., Daliakopoulos, I.N., Tsanis, I.K., 2017. A method to preserve trends in quantile mapping bias correction of climate modeled temperature. Earth Syst. Dyn. https://doi.org/10.5194/esd-8-889-2017.

Gudmundsson, L., Wagener, T., Tallaksen, L.M., Engeland, K., 2012. Evaluation of nine large-scale hydrological models with respect to the seasonal runoff climatology in Europe. Water Resour. Res. 48. https://doi.org/10.1029/2011WR010911 (n/a-n/a).

Hoad, S.P., Russell, G., Lucas, M.E., Bingham, I.J., 2001. The management of wheat, barley, and oat root systems. Adv. Agron. 74, 193–246. https://doi.org/10.1016/S0065-2113(01)74034-5.

Hunt, E.D., Hubbard, K.G., Wilhite, D.A., et al., 2009. The development and evaluation of a soil moisture index. Int. J. Climatol. 29, 747–759. https://doi.org/10.1002/joc.1749.

IGBP-DIS, 2000. Global Gridded Surfaces of Selected Soil Characteristics (IGBP-DIS).

Jacob, D., Kotova, L., Teichmann, C., et al., 2018a. Climate Impacts in Europe Under +1.5 °C Global Warming.

Jacob, D., Kotova, L., Teichmann, C., et al., 2018b. Climate impacts in Europe under +1.5 °C global warming. Earth's Futur. 6, 264–285. https://doi.org/10.1002/2017EF000710.

Jacobs, C.M.J., 1994. Direct Impact of Atmospheric C0 2 Enrichment on Regional Transpiration Direct Effect van de Toenemende Atmosferische C0 2 Concentratie op Regionale Transpiratie. Wageningen Agricultural University.

Jian, J., Ryu, D., Costelloe, J.F., Su, C.H., 2017. Towards hydrological model calibration using river level measurements. J. Hydrol.: Reg. Stud. 10, 95–109.

Jones, C.D., Hughes, J.K., Bellouin, N., et al., 2011. The HadGEM2-ES implementation of CMIP5 centennial simulations. Geosci. Model Dev. 4, 543–570. https://doi.org/10.5194/gmd-4-543-2011.

Julien, B., Naota, H., Ted, V., et al., 2018. Magnitude and robustness associated with the climate change impacts on global hydrological variables for transient and stabilized climate states. Environ. Res. Lett. 13, 64017.

Kong, X., Dorling, S., Smith, R., 2011. Soil moisture modelling and validation at an agricultural site in Norfolk using the Met Office surface exchange scheme (MOSES). Meteorol. Appl. 18, 18–27. https://doi.org/10.1002/met.197.

Koutroulis, A.G., 2019. Dryland changes under different levels of global warming. Sci. Total Environ. 655, 482–511. https://doi.org/10.1016/J.SCITOTENV.2018.11.215.

Koutroulis, A.G., Vrohidou, A.-E.K., Tsanis, I.K., 2011. Spatiotemporal characteristics of meteorological drought for the Island of Crete. J. Hydrometeorol. 12, 206–226. https://doi.org/10.1175/2010JHM1252.1.

Koutroulis, A., Grillakis, M., Daliakopoulos, I., et al., 2015. Cross Sectoral Impacts on Water Availability at +2 °C and +3 °C for east Mediterranean Island States: the Case of Crete.

Koutroulis, A.G., Grillakis, M.G., Tsanis, I.K., Papadimitriou, L., 2016. Evaluation of precipitation and temperature simulation performance of the CMIP3 and CMIP5 historical experiments. Clim. Dyn. https://doi.org/10.1007/s00382-015-2938-x.

Koutroulis, A., Papadimitriou, L., Grillakis, M., et al., 2018a. Simulating hydrological impacts under climate change: implications from methodological differences of a Pan European assessment. Water 10, 1331. https://doi.org/10.3390/w10101331.

Koutroulis, A.G., Grillakis, M.G., Tsanis, I.K., Jacob, D., 2018b. Mapping the vulnerability of European summer tourism under 2 °C global warming. Clim. Chang., 1–15 https://doi.org/10.1007/s10584-018-2298-8.

Koutroulis, A.G., Papadimitriou, L.V., Grillakis, M.G., et al., 2018c. Freshwater vulnerability under high end climate change. a pan-European assessment. Sci. Total Environ. https://doi.org/10.1016/j.scitotenv.2017.09.074.
Kurnik, B., 2017. Economic Losses from Climate-Related Extremes. European Environment Agency (EEA), Denmark.
Lange, S., 2016. EartH2Observe, WFDEI and ERA-Interim Data Merged and Bias-corrected for ISIMIP (EWEMBI).
Lange, S., 2017. Bias correction of surface downwelling longwave and shortwave radiation for the EWEMBI dataset. Earth Syst. Dyn. Discuss., 1–30 https://doi.org/10.5194/esd-2017-81.
Lobell, D.B., Field, C.B., 2007. Global scale climate-crop yield relationships and the impacts of recent warming. Environ. Res. Lett. 2, 014002. https://doi.org/10.1088/1748-9326/2/1/014002.
MacKellar, N.C., Dadson, S.J., New, M., Wolski, P., 2013. Evaluation of the JULES land surface model in simulating catchment hydrology in southern Africa. Hydrol. Earth Syst. Sci. Discuss. 10, 11093–11128. https://doi.org/10.5194/hessd-10-11093-2013.
Manning, C., Widmann, M., Bevacqua, E., et al., 2018. Soil moisture drought in Europe: a compound event of precipitation and potential evapotranspiration on multiple time scales. J. Hydrometeorol. 19, 1255–1271. https://doi.org/10.1175/JHM-D-18-0017.1.
Marsh, T., Cole, G., Wilby, R., 2007. Major droughts in England and Wales, 1800–2006. Weather 62, 87–93. https://doi.org/10.1002/wea.67.
McSweeney, C.F., Jones, R.G., 2016. How representative is the spread of climate projections from the 5 CMIP5 GCMs used in ISI-MIP? Clim. Serv. 1, 24–29. https://doi.org/10.1016/J.CLISER.2016.02.001.
Mika, J., Horváth, S., Makra, L., Dunkel, Z., 2005. The Palmer Drought Severity Index (PDSI) as an indicator of soil moisture. Phys. Chem. Earth 30 (Parts A/B/C), 223–230. https://doi.org/10.1016/J.PCE.2004.08.036.
Milly, P.C.D., Dunne, K.A., 2016. Potential evapotranspiration and continental drying. Nat. Clim. Chang. 6, 946–949. https://doi.org/10.1038/nclimate3046.
Mishra, A.K., Singh, V.P., 2010. A review of drought concepts. J. Hydrol. 391, 202–216.
Mishra, A., Vu, T., Veettil, A.V., Entekhabi, D., 2017. Drought monitoring with soil moisture active passive (SMAP) measurements. J. Hydrol. 552, 620–632. https://doi.org/10.1016/J.JHYDROL.2017.07.033.
Nachtergaele, F., van Velthuizen, H., Verelst, L., et al., 2008. Harmonized World Soil Database (Version 1.0). FAO, Rome, Italy and IIASA, Laxenburg, Austria, p. 2008.
Narasimhan, B., Srinivasan, R., 2005. Development and evaluation of Soil Moisture Deficit Index (SMDI) and evapotranspiration deficit index (ETDI) for agricultural drought monitoring. Agric. For. Meteorol. 133, 69–88. https://doi.org/10.1016/J.AGRFORMET.2005.07.012.
Naumann, G., Alfieri, L., Wyser, K., et al., 2018. Global changes in drought conditions under different levels of warming. Geophys. Res. Lett. 45, 3285–3296. https://doi.org/10.1002/2017GL076521.
Orth, R., Destouni, G., 2018. Drought reduces blue-water fluxes more strongly than green-water fluxes in Europe. Nat. Commun. 9, 3602. https://doi.org/10.1038/s41467-018-06013-7.
Otkin, J.A., Svoboda, M., Hunt, E.D., et al., 2018. Flash droughts: a review and assessment of the challenges imposed by rapid-onset droughts in the United States. Bull. Am. Meteorol. Soc. 99, 911–919. https://doi.org/10.1175/BAMS-D-17-0149.1.
Pacifico, F., Harrison, S.P., Jones, C.D., et al., 2011. Evaluation of a photosynthesis-based biogenic isoprene emission scheme in JULES and simulation of isoprene emissions under present-day climate conditions. Atmos. Chem. Phys. 11, 4371–4389. https://doi.org/10.5194/acp-11-4371-2011.
Papadimitriou, L.V., Koutroulis, A.G., Grillakis, M.G., Tsanis, I.K., 2016. High-end climate change impact on European runoff and low flows - exploring the effects of forcing biases. Hydrol. Earth Syst. Sci. https://doi.org/10.5194/hess-20-1785-2016.
Papadimitriou, L.V., Koutroulis, A.G., Grillakis, M.G., Tsanis, I.K., 2017. The effect of GCM biases on global runoff simulations of a land surface model. Hydrol. Earth Syst. Sci. https://doi.org/10.5194/hess-21-4379-2017.
Penman, H.L., 1948. Natural evaporation from open water, bare soil and grass. Proc. R. Soc. Lond. A 193, 120–145. https://doi.org/10.1098/rspa.1948.0037.
Portmann, F.T., Siebert, S., Döll, P., 2010. MIRCA2000-global monthly irrigated and rainfed crop areas around the year 2000: a new high-resolution data set for agricultural and hydrological modeling. Glob. Biogeochem. Cycles 24. https://doi.org/10.1029/2008GB003435 (n/a-n/a).
Ruosteenoja, K., Markkanen, T., Venäläinen, A., et al., 2018. Seasonal soil moisture and drought occurrence in Europe in CMIP5 projections for the 21st century. Clim. Dyn. 50, 1177–1192. https://doi.org/10.1007/s00382-017-3671-4.
Samaniego, L., Thober, S., Kumar, R., et al., 2018. Anthropogenic warming exacerbates European soil moisture droughts. Nat. Clim. Chang. 8, 421–426. https://doi.org/10.1038/s41558-018-0138-5.
Seneviratne, S.I., Corti, T., Davin, E.L., et al., 2010. Investigating soil moisture-climate interactions in a changing climate: a review. Earth Sci. Rev. 99, 125–161. https://doi.org/10.1016/j.earscirev.2010.02.004.
Sheffield, J., 2004. A simulated soil moisture based drought analysis for the United States. J. Geophys. Res. 109, D24108. https://doi.org/10.1029/2004JD005182.
Sims, A.P., Niyogi D dutta, S., Raman, S., 2002. Adopting drought indices for estimating soil moisture: a North Carolina case study. Geophys. Res. Lett. 29, 24-1–24-4. https://doi.org/10.1029/2001GL013343.
Sivakumar, M., Motha, R., Wilhite, D., Wood, D., 2011. Agricultural Drought Indices Proceedings of an Expert Meeting Murcia, Spain. World Meteorological Organization, Switzerland, p. 2011.
Slevin, D., Tett, S.F.B., Williams, M., 2014. Multi-site evaluation of the JULES land surface model using global and local data. Geosci. Model Dev. Discuss. 7, 5341–5380. https://doi.org/10.5194/gmdd-7-5341-2014.
Sood, A., Smakhtin, V., 2015. Global hydrological models: a review. Hydrol. Sci. J. 60, 549–565. https://doi.org/10.1080/02626667.2014.950580.
Spinoni, J., Naumann, G., Carrao, H., et al., 2014. World drought frequency, duration, and severity for 1951–2010. Int. J. Climatol. 34, 2792–2804. https://doi.org/10.1002/joc.3875.
Spinoni, J., Naumann, G., Vogt, J.V., Barbosa, P., 2015. The biggest drought events in Europe from 1950 to 2012. J. Hydrol. Reg. Stud. 3, 509–524. https://doi.org/10.1016/J.EJRH.2015.01.001.
Sridhar, V., Hubbard, K.G., You, J., et al., 2008. Development of the soil moisture index to quantify agricultural drought and its "user friendliness" in severity-area-duration assessment. J. Hydrometeorol. 9, 660–676. https://doi.org/10.1175/2007JHM892.1.
The Guardian, 2018. Crop failure and bankruptcy threaten farmers as drought grips Europe|Environment|The Guardian. Guardian https://www.theguardian.com/environment/2018/jul/20/crop-failure-and-bankruptcy-threaten-farmers-as-drought-grips-europe, Accessed date: 14 September 2018.
Unnikrishnan, C.K., George, J.P., Lodh, A., et al., 2016. Validation of two gridded soil moisture products over India with in-situ observations. J. Earth Syst. Sci. 125, 935–944. https://doi.org/10.1007/s12040-016-0714-x.
Van den Hoof, C., Lambert, F., 2016. Mitigation of drought negative effect on ecosystem productivity by vegetation mixing. J. Geophys. Res. Biogeosci. 121, 2667–2683. https://doi.org/10.1002/2016JG003625.
Van den Hoof, C., Hanert, E., Vidale, P.L., 2011. Simulating dynamic crop growth with an adapted land surface model – JULES-SUCROS: model development and validation. Agric. For. Meteorol. 151, 137–153. https://doi.org/10.1016/J.AGRFORMET.2010.09.011.
Van den Hoof, C., Vidale, P.L., Verhoef, A., Vincke, C., 2013. Improved evaporative flux partitioning and carbon flux in the land surface model JULES: impact on the simulation of land surface processes in temperate Europe. Agric. For. Meteorol. 181, 108–124. https://doi.org/10.1016/J.AGRFORMET.2013.07.011.
Van Genuchten, M.T., 1980. A closed-form equation for predicting the hydraulic conductivity of unsaturated soils 1. Soil Sci. Soc. Am. J. 44, 892–898.
Van Vuuren, D.P., Edmonds, J., Kainuma, M., et al., 2011. The representative concentration pathways: an overview. Clim. Chang. 109, 5–31. https://doi.org/10.1007/s10584-011-0148-z.
Vörösmarty, C.J., Green, P., Salisbury, J., Lammers, R.B., 2000. Global water resources: vulnerability from climate change and population growth. Science 289, 284–288. https://doi.org/10.1126/SCIENCE.289.5477.284.
Vrochidou, A.-E.K., Tsanis, I.K., Grillakis, M.G., Koutroulis, A.G., 2013. The impact of climate change on hydrometeorological droughts at a basin scale. J. Hydrol. https://doi.org/10.1016/j.jhydrol.2012.10.046.
Walsh, B., Ciais, P., Janssens, I.A., et al., 2017. Pathways for balancing CO2 emissions and sinks. Nat. Commun. 8, 14856. https://doi.org/10.1038/ncomms14856.
Walters, D.N., Williams, K.D., Boutle, I.A., et al., 2014. The Met Office unified model global atmosphere 4.0 and JULES global land 4.0 configurations. Geosci. Model Dev. 7, 361–386. https://doi.org/10.5194/gmd-7-361-2014.
Walters, D., Boutle, I., Brooks, M., et al., 2017. The Met Office unified model global atmosphere 6.0/6.1 and JULES global land 6.0/6.1 configurations. Geosci. Model Dev. 10, 1487–1520. https://doi.org/10.5194/gmd-10-1487-2017.
Wang, A., Lettenmaier, D.P., Sheffield, J., et al., 2011. Soil moisture drought in China, 1950–2006. J. Clim. 24, 3257–3271. https://doi.org/10.1175/2011JCLI3733.1.
Warszawski, L., Frieler, K., Huber, V., et al., 2014. The inter-sectoral impact model Intercomparison project (ISI–MIP): project framework. Proc. Natl. Acad. Sci. 111, 3228–3232. https://doi.org/10.1073/pnas.1312330110.
Watanabe, M., Suzuki, T., O'ishi, R., et al., 2010. Improved climate simulation by MIROC5: mean states, variability, and climate sensitivity. J. Clim. 23, 6312–6335. https://doi.org/10.1175/2010JCLI3679.1.
Webber, H., Ewert, F., Olesen, J.E., et al., 2018. Diverging importance of drought stress for maize and winter wheat in Europe. Nat. Commun. 9, 4249. https://doi.org/10.1038/s41467-018-06525-2.
Williams, C., Quaife, T., 2016. The use of HydEOMEx Data to Validate a Land Surface Model Over the UK.
Williges, K., Mechler, R., Bowyer, P., Balkovic, J., 2017. Towards an assessment of adaptive capacity of the European agricultural sector to droughts. Clim. Serv. 7, 47–63. https://doi.org/10.1016/j.cliser.2016.10.003.
Yang, H., Wang, H., Fu, G., et al., 2017. A modified soil water deficit index (MSWDI) for agricultural drought monitoring: case study of Songnen Plain, China. Agric. Water Manag. 194, 125–138. https://doi.org/10.1016/J.AGWAT.2017.07.022.
Yee, M., Walker, J.P., Dumedah, G., et al., 2013. Towards land surface model validation from using satellite retrieved soil moisture. 20th International Congress on Modelling and Simulation (MODSIM2013).
Yevjevich, V., 1967. An objective approach to definitions and investigations of continental hydrologic driughts. Hydrology Papers. Colorado State University, Fort Collins Colorado.
Zaherpour, J., Gosling, S.N., Mount, N., et al., 2018. Worldwide evaluation of mean and extreme runoff from six global-scale hydrological models that account for human impacts. Environ. Res. Lett. 13, 065015. https://doi.org/10.1088/1748-9326/aac547.
Zhang, Y., Gong, J., Sun, K., et al., 2017. Estimation of soil moisture index using multi-temporal Sentinel-1 images over Poyang Lake ungauged zone. Remote Sens. 10, 12. https://doi.org/10.3390/rs10010012.
Zhao, F., Veldkamp, T.I.E., Frieler, K., et al., 2017. The critical role of the routing scheme in simulating peak river discharge in global hydrological models. Environ. Res. Lett. 12, 075003. https://doi.org/10.1088/1748-9326/aa7250.
Zhou, H., Wu, J., Geng, G., et al., 2017. Enhancing the ability of a soil moisture-based index for agricultural drought monitoring by incorporating root distribution. JAWRA. J. Am. Water Resour. Assoc. 53, 1409–1423. https://doi.org/10.1111/1752-1688.12573.